Efficient solid-phase RNA extraction using carbon nanomaterials

A M Videira, P L Ferreira, M J Sampaio, P. Serp, J L Faria, C G Silva, F Sousa

Colloids and Surfaces A: Physicochemical and Engineering Aspects 704 (2025) 135532

Contents lists available at ScienceDirect

Colloids and Surfaces A: Physicochemical and Engineering Aspects

journal homepage: www.elsevier.com/locate/colsurfa

Efficient solid-phase RNA extraction using carbon nanomaterials

A.M. Videira [a,1], P.L. Ferreira [a,1], M.J. Sampaio [b,c], Philippe Serp [d], J.L. Faria [b,c], C.G. Silva [b,c,*], F. Sousa [a,*]

[a] CICS-UBI – Health Sciences Research Centre, University of Beira Interior, Av. Infante D. Henrique, Covilhã 6200-506, Portugal
[b] LSRE-LCM – Laboratory of Separation and Reaction Engineering – Laboratory of Catalysis and Materials, Faculty of Engineering, University of Porto, Rua Dr. Roberto Frias, Porto 4200-465, Portugal
[c] ALiCE – Associate Laboratory in Chemical Engineering, Faculty of Engineering, University of Porto, Rua Dr. Roberto Frias s/n, Porto 4200-465, Portugal
[d] Laboratoire de Chimie de Coordination, UPR CNRS 8241, Composante ENSIACET, Université de Toulouse, UPS-INP LCC, 4 Allée Emile Monso, BP 44362, Cedex 4, Toulouse 31030, France

HIGHLIGHTS

- Simple, cost-effective RNA recovery from *E. coli* extracts using carbon materials.
- CNT-N-ox and CNF-ox allowed good adsorption and recovery of RNA.
- Method recovered RNA free from DNA and protein contamination.
- Materials were reusable, maintaining RNA adsorption capacity over four cycles.

GRAPHICAL ABSTRACT

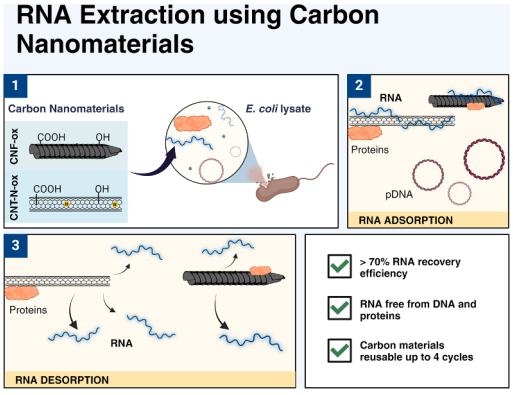

ARTICLE INFO

Keywords:
RNA-based therapeutics
RNA capture
Carbon materials
Adsorbents
Solid-phase extraction

ABSTRACT

Recent research highlights RNA's therapeutic potential in nucleic acid-based therapies. However, effective RNA recovery and purification remain challenging due to similar impurities affecting therapeutic outcomes. Traditional RNA isolation methods are often slow, inefficient, and involve toxic reagents. Carbon-based materials offer a promising alternative as adsorbents for nucleic acids due to their excellent mechanical and chemical properties. This study describes an efficient, simple, and cost-effective method for RNA recovery from complex *Escherichia coli* extracts using carbon materials with different structures and surface modifications. RNA adsorption and desorption screening experiments were performed using different carbon materials. N-doped CNTs (CNT-N-ox) and carbon nanofibers (CNF-ox), both oxidized with HNO_3, showed RNA adsorption capacities of 42 % and 55 %, respectively, also allowing effective RNA desorption (81 % and 72 %, respectively). Additionally, the materials demonstrated reusability, maintaining RNA adsorption capacity over four cycles. The selectivity of the materials enabled a simple method to recover RNA free from DNA contamination by performing three consecutive cycles.

* Corresponding authors.
E-mail addresses: cgsilva@fe.up.pt (C.G. Silva), fani.sousa@fcsaude.ubi.pt (F. Sousa).
[1] Both authors contributed equally.

https://doi.org/10.1016/j.colsurfa.2024.135532
Received 26 August 2024; Received in revised form 6 October 2024; Accepted 8 October 2024
Available online 10 October 2024

Moreover, no contaminating protein was found in the recovered sample. The analysis by circular dichroism also revealed that RNA maintained its integrity and stability when recovered from these materials. Overall, the study demonstrates the potential of carbon materials for efficient RNA capture and pre-purification.

1. Introduction

RNA-based therapeutics have become a rapidly growing field with exciting progress in different areas and targeting different diseases [4]. In recent years, new biological roles were discovered, encompassing regulatory and enzymatic functions. As such, RNA has become a potential biomarker for the diagnosis of certain diseases or a pharmaceutical agent, modulating the expression levels of pivotal proteins involved in diverse cellular mechanisms [8].

RNAs can be obtained by different methods, namely, by *in vitro* transcription (enzymatic production), chemical synthesis, and recombinant production. Among these procedures, recombinant production can stand out as a cost-efficient process with significant potential for large-scale production. It also demonstrates superior performance in preserving RNAs' structure and biological functions, potentially reducing the risk of immunogenic responses [4,5,8]. Regardless, RNA capture and purification processes are critical as they serve as the starting point for the development of high-quality biopharmaceutical products [20]. In addition, maximizing RNA recovery yield is another major challenge as it is intended to end up with a final RNA sample in high quantity and free of impurities. Considering a biotechnological process, which can offer higher productivity levels, the diversity of biomolecules arising from the producer host creates additional challenges. Upon cell lysis, the resulting material comprises only 21 % of total RNA, whereas 55 % consists of proteins, and 3 % of pDNA [32]. Historically, strong denaturants have been used in RNA isolation [33]. For example, the conventional method for RNA isolation relies on a combination of guanidinium thiocyanate, phenol, and chloroform, as established by Chomczynski and Sacchi in 1987 [9]. This mixture separates into two phases, with the total RNA remaining in the upper aqueous phase, while DNA and proteins remain in the interphase or lower organic phase. Although obtaining high yields and purity, this method is often laborious and requires the use of toxic reagents and organic solvents to achieve the separation [1]. Another approach for RNA purification, which is commonly employed in most commercially available kits, involves adsorption techniques using silica-based membranes in the presence of chaotropic salts. This method is popular due to its simplicity, speed, and efficiency [36]. However, silica-based membranes exhibit a high affinity for both RNA and DNA. The strong interaction with DNA is due to the negatively charged DNA backbone, which is attracted by the positively charged silica particles [34]. As a result, without additional steps, DNA can be a significant issue during RNA purification. To address this, many commercial kits include DNase treatment to selectively degrade and remove contaminating DNA, ensuring the purity of the RNA. Nevertheless, the effectiveness of DNase can vary, and additional optimization may be required in some protocols to achieve the desired RNA purity. Moreover, residual DNase itself can become a contaminant, causing difficulties in the process. Many methods are being developed to circumvent the various challenges of RNA purification, but new perspectives should be envisioned to find more efficient procedures and support market demand.

The use of carbon-based adsorbents for solid-phase extraction (SPE) emerges as a highly promising method to overcome these obstacles [33]. These materials exhibit a range of favorable characteristics, such as a high specific surface area-to-volume ratio, exceptional mechanical strength and durability, and versatile electrical and thermal conductivity [6]. These properties render them exceptionally well-suited as adsorbents, and they are being studied for a wide range of applications. They prove effective in removing hazardous substances from industrial wastewater [12,27,28], and have also been studied as drug delivery systems and nanosensors [19]. In particular, carbon nanotubes (CNTs) have gained well-deserved popularity in this field due to their excellent adsorptive capabilities, emerging as a promising option worthy of further study for the capture of nucleic acids, particularly RNA [14].

This study, presentes a straightforward approach for capturing and recovering RNA from bacterial lysate samples using carbon nanomaterials. This procedure is characterized by its simplicity, and effectiveness, avoiding the need to employ any hazardous organic solvent. Various carbon nanomaterials were harnessed to selectively capture RNA from complex bacterial lysates, taking advantage of the structural differences between RNA and DNA. It was also comprehensively characterized the adsorption capacity through Langmuir adsorption isotherms, optimizing desorption processes and confirming the materials' reusability. Finally, RNA integrity post-procedure was validated by circular dichroism analysis.

This innovative method not only promises efficient RNA capture but also underscores its versatility, further advancing the field of nucleic acid extraction and purification.

2. Materials and methods

2.1. Materials

Different carbon nanomaterials were employed to perform the solid phase dispersive extraction method (d-SPE) for RNA capture and recovery. Carbon nanofibers (CNF) were synthesized via catalytic chemical vapor deposition (CVD) using a ternary oxide catalyst and ethylene as the carbon source in a fluidized bed reactor, as previously described [30]. CNF sample was purified using hydrochloric acid (37 wt%, HCl, Sigma–Aldrich) for 12 h.

Pristine carbon nanotubes (CNT-P) were synthesized by a catalytic CVD process in a fluidized bed reactor using ethylene as the carbon source at 650 ºC, as described elsewhere [26]. Then, CNT-P sample was purified using 50 vol% of sulfuric acid (99.9 wt%, H_2SO_4, Sigma–Aldrich) at 120 °C for 3 h.

For nitrogen-doping, CNT-P sample was exposed to acetonitrile/N_2 flow thermal treatment at 650ºC. The resulting material was labelled as CNT-N.

Posterior oxidation for CNT-N and neat CNF was performed with nitric acid (65 wt% HNO_3, Sigma–Aldrich) at 120 °C for 3 hours under reflux. After cooling, the suspensions were washed with distilled water until neutral pH and dried at 130 °C for 12 h. Finally, the resulting materials were designated as CNT-N-ox and CNF-ox, respectively.

The specific surface areas (S_{BET}) of the carbon materials were obtained by N_2 adsorption–desorption isotherms at −196 °C using a Quantachrome Nova 4200e apparatus. The S_{BET} for CNF-ox and CNT-N-ox obtained were 103 ± 5 $m^2\ g^{-1}$ and 115 ± 5 $m^2\ g^{-1}$, respectively.

The diameter of CNT-P and CNF was determined by transmission electron microscopy using a TEM-FEI Tecnai-G2–20-FEI 2006 microscope, being 20 and 70 nm, respectively.

The different adsorption and desorption/regeneration experiments performed in this work required the use of several reagents, namely ammonium sulfate ($(NH_4)_2SO_4$), Tween-20 ($C_{58}H_{114}O_{26}$), sodium hydroxide (NaOH), sodium chloride (NaCl) commercialized by Panreac (Barcelona, Spain), Triton X-100 ($C_{16}H_{26}O_2$) from Thermo Fisher Scientific Inc. (Waltham, USA) and tris(hydroxymethyl)aminomethane (Tris) from Merck (Darmstadt, Germany). All solutions were prepared with ultrapure deionized water and purified with Merck Millipore's Milli-Q® system (Burlington, MA, USA).

For *E. coli* DH5α growth, "Luria-Bertani" (LB) agar medium from

Pronalab (Mérida, Mexico), yeast extract and tryptone from Biokar (Beauvais, France), glycerol from Himedia (Einhausen, Germany), potassium hydrogen phosphate (K_2HPO_4) from Panreac (Barcelona, Spain), potassium dihydrogen phosphate (KH_2PO_4) from Sigma-Aldrich (St. Louis, Missouri, USA) and the antibiotic kanamycin from Thermo Fisher Scientific Inc. (Waltham, EUA) have been used.

For nucleic acids extraction, the reagents used were guanidine thiocyanate, N-Lauroylsarcosine sodium salt, sodium citrate, and isoamyl alcohol from Sigma-Aldrich (St. Louis, Missouri, USA), isopropanol from Thermo Fisher Scientific Inc. (Waltham, USA), β-mercaptoethanol from Merck (Whitehouse Station, USA). All mentioned solutions were prepared with 0.05 % diethyl pyrocarbonate treated water (DEPC) from Fluka, Sigma-Aldrich (St. Louis, Missouri, USA). For plasmid DNA extraction, the NZYMaxiprep kit from NZYTech Genes and Enzymes (Lisbon, Portugal) was used. For the lysate preparation by alkaline cell lysis, solution A composed of Tris from Merck (Darmstadt, Germany) and EDTA from Sigma-Aldrich (St. Louis, Missouri, USA); solution B composed of NaOH and SDS from Panreac (Barcelona, Spain); and solution C with potassium acetate from Panreac (Barcelona, Spain) were previously prepared.

To verify the integrity and purity of the nucleic acids in the electrophoresis, 1 % agarose gel electrophoresis was used with GRS Agarose LE and Green Safe from Grisp (Porto, Portugal).

Dye Reagent Concentrate and bovine serum albumin (BSA) from Bio-Rad (California, USA) were used for protein quantification.

2.2. Methods

2.2.1. Bacterial growth conditions and nucleic acids production

RNA and pDNA were obtained from an *E. coli* DH5α culture previously transformed with the plasmid pBHSR1-RM, which contains the sequence of human pre-miRNA29b and has a total size of 4065 base pairs (bp) [24], as well as the plasmid pUC19, with a total size of 2686 bp, from Invitrogen (Waltham, USA). Bacterial growth was carried out at 37 ℃ using Terrific Broth medium (12 g/L tryptone, 24 g/L yeast extract, 4 mL/L glycerol, 0.017 M KH_2PO_4, and 0.072 M K_2HPO_4) supplemented with 50 μg/mL kanamycin. The growth was kept for 8 h for low molecular weight RNA production or 16 h for pDNA production. Cells were recovered by centrifugation at 3900 G for 10 min at 4 ℃ and stored at −20 ℃.

2.3. Low molecular weight RNA extraction

RNA extraction, yielding molecules ranging from 50 to 300 nucleotides, was performed using the method of acid guanidinium thiocyanate-phenol-chloroform [10]. First, the pellets previously stored at −20 ℃ were thawed and resuspended in 0.8 % NaCl, followed by centrifugation at 6000 G for 10 min at 4 ℃. After that, the supernatant was discarded, and the resulting cell pellets were resuspended in 5 mL of solution D, which corresponds to the denaturing solution, composed of 4 M guanidinium thiocyanate, 0.5 % sodium N-lauroyl sarcosinate, 0.025 M sodium citrate pH 7, and 0.1 M β-mercaptoethanol, and incubated on ice for 10 min. The next step consists of adding 0.5 mL of 2 M sodium acetate pH 4 and 5 mL of phenol to the suspensions and homogenizing very carefully at each step. Then, a chloroform/isoamyl alcohol mixture (49:1) was prepared, and 1 mL was added to the suspension, followed by vigorous shaking and incubation on ice for 15 min. After centrifugation, two aqueous phases are formed, the upper phase being rich in RNA, while the bottom phase is rich in DNA. For this reason, the upper phase should be transferred very carefully to new tubes to avoid possible contamination with DNA. To these new tubes, 5 mL of isopropanol was added to precipitate the RNA, and the suspension was centrifuged at 10,000 G for 20 min at 4 ℃. After discarding the supernatant, RNA reprecipitation was performed by dissolving the RNA pellets in 1.5 mL of solution D and then 1.5 mL of isopropanol, followed by centrifugation at 10,000 G for 10 min at 4 ℃. The supernatant was discarded, and the resulting pellets were resuspended in 2.5 mL of 75 % ethanol in DEPC water to wash the RNA. Next, the samples were incubated at room temperature for 10–15 min to dissolve possible residual traces of guanidinium. After that, the suspension was centrifuged at 10,000 G for 5 min at 4 ℃. The supernatant was discarded, and the resulting pellets were dried for 5–10 minutes at room temperature. Finally, the RNA pellets were dissolved in 1 mL of DEPC-treated water and incubated at room temperature for 10–15 min to ensure complete solubilization. RNA concentration was measured using a Nano Photometer (IMPLEN, United Kingdom), and RNA integrity was verified by agarose gel electrophoresis. Then, the samples were stored at −80 ℃ until the moment of use.

2.4. Plasmid DNA extraction

For pDNA extraction, the NZYMaxiprep kit (NZYTech, Portugal) was used, according to the protocol provided by the manufacturer. The protocol describes the purification of pDNA using an anion exchange resin. The process involves alkaline lysis of bacterial cells, followed by binding of pDNA to the resin under appropriate salt and pH conditions. Impurities are removed during the washing step, and pDNA is finally eluted with a high salt buffer. The resulting pDNA is then concentrated through isopropanol precipitation. The final pDNA samples were quantified using a NanoPhotometer (IMPLEN, UK), and the integrity of the samples was verified by agarose gel electrophoresis, with the samples being stored at −20 °C.

2.5. Cell lysate extraction

To obtain a complex cell lysate extract composed of pDNA, gDNA, RNA, and proteins, a modified alkaline lysis method was used, as previously described [11]. The bacterial pellets were resuspended in 10 mL of solution A composed of 50 mM Tris-HCl, and 10 mM EDTA at pH 8.0, and then the volume was divided into two new lysis tubes by adding 5 mL of solution B (200 mM NaOH and 1 % (w/v) SDS), followed by 5 min incubation at room temperature to promote cell lysis. To neutralize the samples, 5 mL of solution C (3 M potassium acetate at pH 5.0) was added and incubated on ice for 20 min. Next, the tubes were centrifuged twice at 20,000 G for 30 min at 4 °C to eliminate major cellular debris, and the supernatant was stored at −80 °C until use.

2.6. Dispersive solid-phase extraction (d-SPE) of RNA using carbon materials

In the present work, the d-SPE method was applied primarily for the capture and recovery of RNA from complex *E. coli* lysates using different carbon-based materials. For this purpose, an optimization of the experimental parameters was required as an initial screening to determine the most influential factors affecting the performance of the method. These parameters are described in detail in the "Results" section. The bioseparation process was divided into 3 main steps: equilibrium step, adsorption step, and desorption step, as schematically represented in Fig. 1.

In the equilibration step, 1 mg of each carbon material under study was equilibrated with an appropriate equilibration buffer. For this, different solutions were tested by adjusting the type and concentration of salt and the pH to make a correct choice of the equilibrium buffer to be used. After that, agitation was performed for 20 min with subsequent centrifugation at 9000 G for 4 min to remove the aqueous phase.

In the adsorption step, the sample to be adsorbed/extracted, in this case, enriched-RNA sample, was diluted in the equilibrium buffer and subsequently applied to the carbon material. The mixture was kept in agitation for 20 min at room temperature (approximately 25 ℃) to allow the adsorption of the RNA to the carbon material. After that, an additional centrifugation at 9000 G for 4 min was performed to separate the solid phase from the aqueous phase (supernatant). The recovery of this supernatant is very important because it will allow us to evaluate the

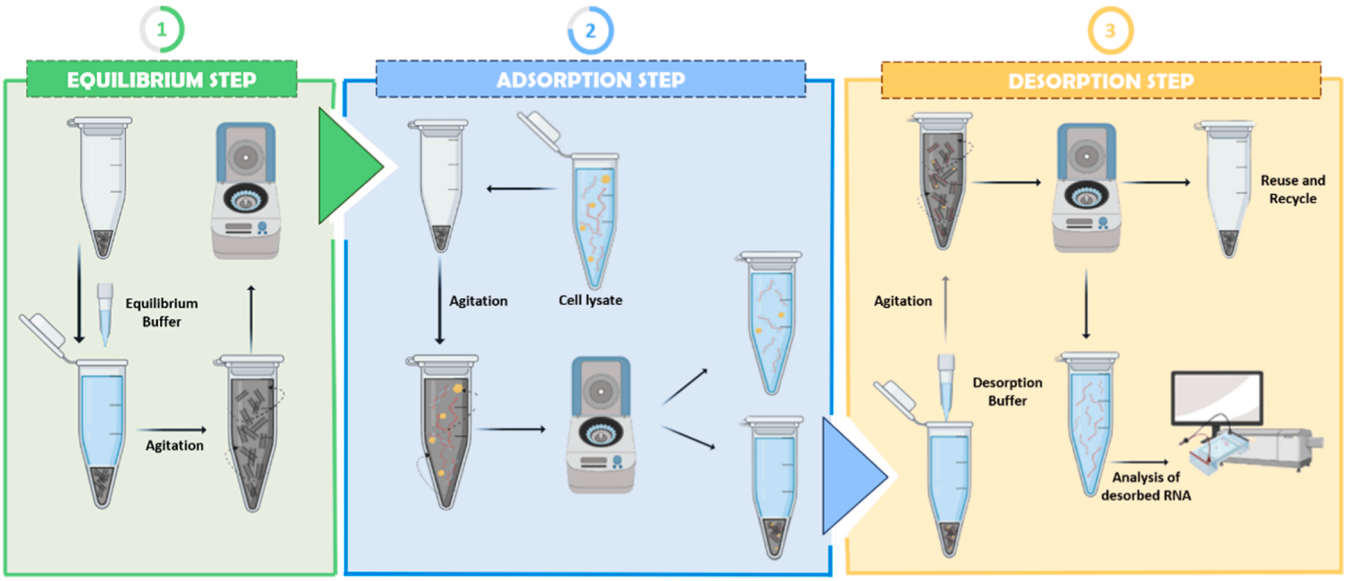

Fig. 1. Overview of the applied d-SPE method.

behavior and, consequently, confirm the efficiency of the RNA adsorption. Thus, the absorbance of the supernatant was measured using a Nano Photometer (IMPLEN, UK), and an agarose gel electrophoresis was performed.

Lastly, in the desorption step, an appropriate elution buffer was applied to allow the recovery of the RNA that was adsorbed onto the carbon material. Similar to the choice of equilibrium buffer, the elution buffer required initial screening of different solutions, varying in salt type and concentration, and pH. This mixture was agitated for 20 min and then centrifuged at 9000 G for 4 min to recover the aqueous phase containing the desorbed RNA. To assess the purity and integrity of the RNA, agarose gel electrophoresis and circular dichroism spectrum analysis were performed using Jasco J-815 spectropolarimeter (Jasco, Easton, MD, USA). In parallel, to ensure the complete removal of the elution buffer, 3 washes with deionized water were performed. Finally, the carbon material was oven-dried at 37 °C for 24 h and stored for later use. In order to recycle and reuse the carbon material for new RNA adsorption/desorption cycles, different regeneration approaches were adopted to study the most suitable regeneration strategy to be applied.

2.7. Adsorption experiments

For the adsorption isotherm studies, a small RNA (sRNA) sample with different concentrations (10, 20, 30, 40, and 50 μg/mL RNA) were used as a model. The samples were added to the carbon materials, and the equilibrium time was fixed at 20 min, which was sufficient to adsorb RNAs, according to the preliminary experiments. The absorbance at 260 nm was measured in a NanoPhotometer (IMPLEN, UK). The blank used in the experiment was the equilibrium buffer. The amount of RNA adsorbed was calculated from the measurement of the absorbance at 260 nm of the supernatants recovered after the adsorption step. Each experiment was performed in triplicate under identical conditions. The RNA adsorption at equilibrium, qe (mg/g), was calculated by the equation:

$$qe = V * \frac{C_0 - C_e}{m} \quad (1)$$

where C_0 and Ce are the initial and equilibrium concentrations of RNA (mg/L) in solution, respectively; V is the volume of the solution (L), and m is the mass of the adsorbent (g).

2.8. Agarose gel electrophoresis

The content of nucleic acids in the supernatants recovered after the adsorption and desorption steps was evaluated by horizontal gel electrophoresis using a 1 % agarose gel stained with 0.012 μL/mL of GreenSafe. Electrophoresis was performed at 120 V for 30 min in TAE buffer (40 mM Tris base, 20 mM acetic acid, 1 mM EDTA pH 8). The gels were visualized and analyzed using ultraviolet (UV) light with the Uvitec Cambridge Fire-Reader UV system (UVITEC Cambridge, Cambridge, UK).

2.9. Circular Dichroism spectroscopy

Circular Dichroism (CD) experiments were performed to evaluate the stability of the recovered RNA after the d-SPE procedure. The CD was conducted in the Jasco J-815 spectropolarimeter (Jasco, Easton, MD, USA), using a Peltier-type temperature control system and a quartz cell with a 1 mm optical path. The CD spectra were obtained at a constant temperature of 20℃, scanning speed of 50 nm/min, with a response time of 1 sec within a wavelength range of 200–320 nm. The samples subjected to CD analysis were the pure sRNAs (control) and the RNA samples recovered from carbon materials. All samples were prepared in DEPC-treated water. Three scans were measured per spectrum to improve the signal-to-noise ratio, and the spectra were smoothed using the smooth tool in Origin 2021 software.

2.10. Total protein quantification

Standard Bio-Rad Protein Assay (Bio-Rad, California, USA) was used to determine the total protein concentration present in the samples recovered from the carbon materials after 3 consecutive cycles. For this, a calibration curve was designed, using BSA as standard protein, in the linear range of 0.05–0.5 mg/mL. Next, the dye reagent was prepared by diluting 1 part of dye reagent to 4 parts of deionized distilled water, with subsequent filtration to remove possible particulate material. Each standard and sample solutions were prepared in a 96-well microplate, in triplicate using 10 μL of sample and 200 μL of dye reagent. Then, the absorbance of the microplate was recorded at 595 nm in an xMarkTM Microplate Absorbance Spectrophotometer (Bio-Rad, USA), and the amount of protein was calculated using the previously designed calibration curve, shown in Supporting Information.

3. Results and discussion

3.1. Screening of adsorption and desorption conditions

Carbon materials with different surface chemistry and textural properties were evaluated as RNA adsorbents. These materials included CNT-P, CNT-N, CNT-N-ox, CNF and CNT-N-ox. Different equilibration/elution buffers, varying the ionic strength, were evaluated to find the best conditions for the adsorption and desorption of RNA. Aliquots containing 1 mg of each carbon material were prepared, and a model sample of low molecular weight RNA (50 μg/mL) was diluted in the respective equilibration buffer.

3.1.1. RNA adsorption

First, an equilibration buffer with low ionic strength (10 mM Tris-HCl pH 8.0) was used to establish the conditions that can promote electrostatic interactions if these forces are eventually present. Under these experimental conditions, a considerably low RNA adsorption was achieved for all carbon materials, and thus, no RNA recovery was attained (results not shown). This phenomenon may occur due to the lack of surface chemical groups on non-functionalized carbon materials. On the other hand, treatment with HNO_3 promotes the incorporation of a large number of oxygen-containing species, especially carboxylic acid functional groups (-COOH) [2]. Several studies reported in the literature have shown that the carboxylic groups generated during the oxidation of various carbon-based materials cause an increase in surface negative charge, which, in this case, will not favor the interaction with RNA. In 2013, Hamilton and co-workers proceeded to oxidize the surface of multi-walled carbon nanotubes (MWCNTs) with HNO_3 and measured the zeta potential of both pristine oxidized MWCNTs, obtaining the values of −9.76 mV and −13.8 mV, respectively. The reason was that the -COOH groups could generate the negatively charged COO^- species due to the low isoelectric point, leading to a more negative surface [18]. On the other hand, the phosphate backbone of RNA has one negative charge per residue, making RNA a highly negative charged molecule [22]. As such, the lack of established electrostatic interactions can be attributed to the electrostatic repulsion between the negatively charged surface of the oxidized carbon-based materials and the negatively charged RNA.

Afterwards, some changes were performed in the experimental conditions, expecting to promote hydrophobic interactions. This was accomplished by increasing the ionic strength in the equilibration buffer, by adding 1.5 M of ammonium sulfate. As observed in Fig. 2, this resulted in an increase in the adsorption of RNA across all the materials studied. CNT-P enabled complete RNA adsorption, corroborating the results previously obtained in the group with pristine MWCNTs [14]. On the other hand, unmodified CNF shows an adsorption capacity of merely 29.2 %. In parallel, the RNA adsorption capacity of carbon materials was highly influenced by the surface chemistry. The surface of CNT-P is highly hydrophobic, allowing for strong adsorption of RNA via π-π and hydrophobic interactions. Doping carbon nanotubes with nitrogen leads to a change in the polarity and wettability of the material. Thus, the introduction of these hydrophilic moieties implies a reduction of hydrophobic regions, thus compromising RNA capture through these interactions. As can be seen in Fig. 2, there was a reduction of approximately 23 % in the RNA adsorption capacity of the N-doped CNTs in comparison with CNT-P. These results may be rationalized due to the more polarized graphitic surfaces in CNT-N, as the presence of nitrogen can significantly affect the π electron distribution on the surfaces of the materials. In 2014, a study by Arenal and co-workers demonstrated that the nitrogen electrons became relatively localized and disrupted local conjugation, reducing local π contributions [3]. Hence, this could help in understanding the low percentage of RNA adsorption by CNT-N-ox (35 %), as the π-π interactions between the material and RNA could be affected.

A curious result was obtained from the adsorption of RNA on CNF and CNF-ox. Contrary to CNTs CNF-ox presented an increase in RNA adsorption of 17 % when compared to carbon fibers without any surface modification. In 2003, a study published by Pamula and co-workers demonstrated that HNO_3 oxidative treatment of carbon fibers resulted not only in an increase in oxygen-containing functional groups on the surface of the material but also in an increase in the microporosity of the fibers [23]. This increase in the porosity of the CNFs may result in the increase in RNA adsorption on CNF-ox. However, it is important to note that, to the best of our knowledge, there are no reports in the literature about the adsorption of nucleic acids to carbon fibers, so more studies are needed on this subject.

Finally, it was observed that CNT-N-ox and CNF-ox exhibited higher RNA desorption and recovery capacity than the untreated materials, and for this reason, they were selected to proceed to the remaining assays.

3.1.2. Effect of ionic strength on RNA adsorption

Following the selection of hydrophobic interactions as the preferred mechanism for promoting RNA adsorption to the studied carbon materials, the impact of ionic strength on RNA capture by CNT-N-ox and CNF-ox materials was investigated. Typically, separation based on hydrophobic interactions involves the adsorption of hydrophobic molecules using a mobile phase with high ionic strength. To investigate this effect, the concentration of $(NH_4)_2SO_4$ in the adsorption buffer was increased to 2 M and to 2.5 M, both in 10 mM Tris-HCl pH 8. This allowed for a comparative analysis with the initially employed buffer, which contained 1.5 M $(NH_4)_2SO_4$ in 10 mM Tris-HCl pH 8. The results illustrated in Fig. 3 demonstrate a general trend consisting of an increase in the RNA adsorption capacity for both tested materials when increasing the concentration of $(NH_4)_2SO_4$, as anticipated. Particularly, raising the concentration of $(NH_4)_2SO_4$ to 2 M led to a moderate increase in RNA

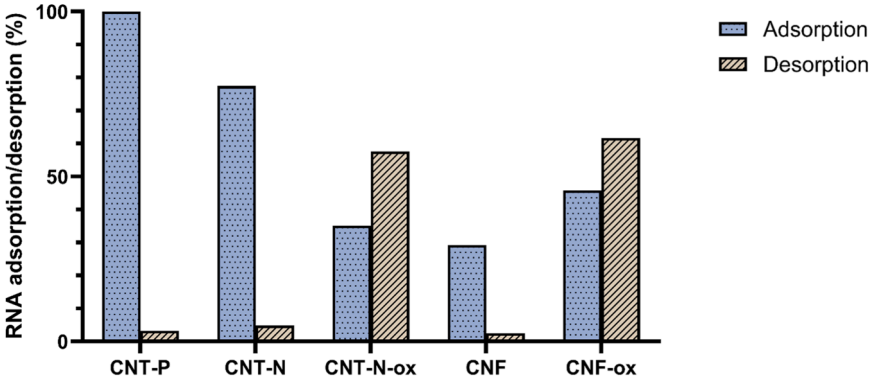

Fig. 2. RNA adsorption and desorption capacity of different carbon-based materials when hydrophobic interactions are promoted (1.5 M $(NH_4)_2SO_4$ in 10 mM Tris-HCl pH 8). The percentage of desorption was determined in relation to the corresponding RNA adsorption.

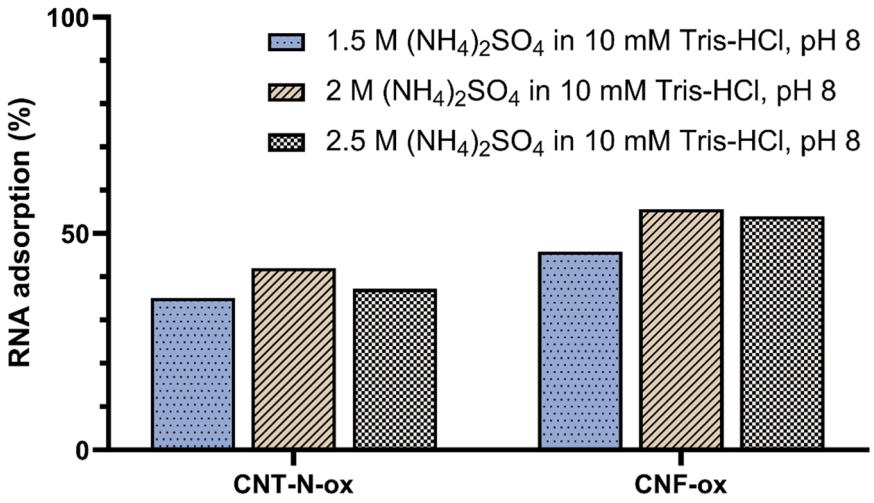

Fig. 3. RNA adsorption capacity of CNT-N-ox and CNF-ox using buffers with different ionic strength.

adsorption, resulting in a 6.9 % increase for CNT-N-ox and 9.9 % increase for CNF-ox. Considering these results, the concentration of 2 M of ammonium sulfate in the adsorption buffer was established for further studies.

3.1.3. *RNA adsorption Isotherms*

The analysis of adsorption isotherms holds significant importance as it provides insights into the distribution of molecules between the liquid and solid phases when the adsorption process attains equilibrium. This information allows the characterization of the RNA adsorption capacity of both materials. To investigate the adsorption isotherms, it was maintained a constant solution volume (1 mL), a fixed amount of adsorbent (1 mg), and a consistent contact time between the adsorbent and adsorbate (20 min), while varying the initial RNA concentration within the range of 10–50 μg/mL. According to Giles and co-workers, the Langmuir isotherm is one of the best known and occurs in most cases of adsorption [16]. According to this model, when the monolayer coverage of the molecules on the adsorbent surface is completed without interaction between the adsorbed molecules, this will be the maximum adsorption capacity [16]. The Langmuir equation (Eq. 2) in non-linearized form is represented by:

$$qe = \frac{K_L * q_{\max} * C_e}{1 + \quad K_L * C_e} \tag{2}$$

where qe (mg/g) and Ce (mg/L) are the amount of RNA adsorbed at equilibrium and RNA concentration at equilibrium (mg/L), respectively. q_{max} (mg/g) is the RNA maximum adsorption capacity, and K_L is the Langmuir equilibrium constant (L/mg) that is related to the free energy of adsorption and describes the affinity of the adsorbate for the adsorbent [17]. Fig. 4 depicts the adsorption isotherms of RNA on N-doped CNTs oxidized with HNO_3 and on carbon fibers oxidized with HNO_3. The experimental data are represented as symbols, and the Langmuir model is represented by solid lines. The Langmuir parameters, as determined through the fitting, are presented in Table 1.

Considering Table 1, when comparing the determination coefficients

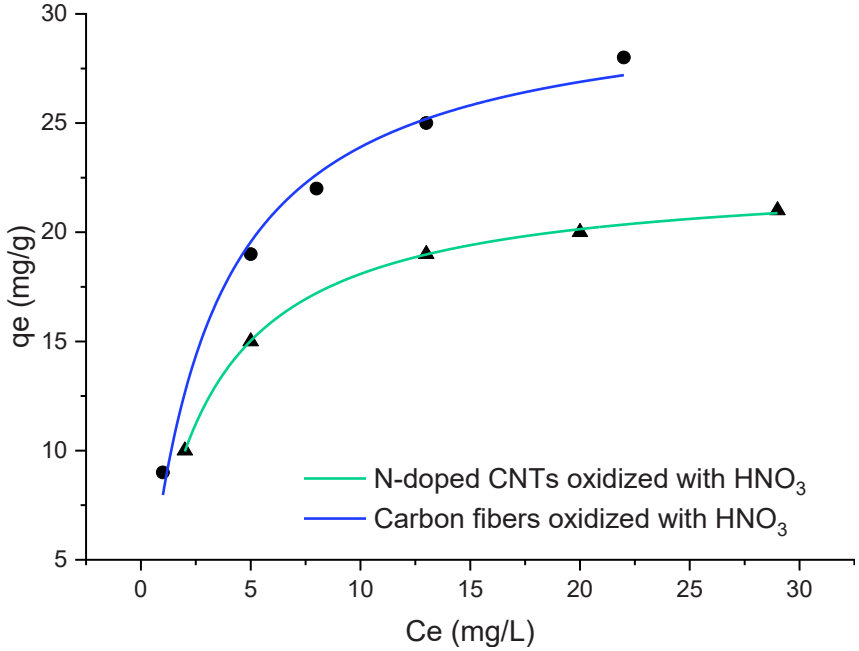

Fig. 4. RNA adsorption isotherms when hydrophobic interactions are promoted (2 M $(NH_4)_2SO_4$ in 10 mM Tris-HCl pH 8). The green curve is representative of RNA adsorption onto the CNT-N-ox, while the blue curve is representative of RNA adsorption onto the CNF-ox.

Table 1
Langmuir parameters obtained by fitting the data in Fig. 4.

Carbon material	R^2	q_{max} (mg/g)	K_L (L/mg)
CNT-N-ox	0.9995	22.7	0.3907
CNF-ox	0.9884	30.8	0.3501

(R^2), it can be concluded that this model proved to be quite adequate to describe the RNA adsorption processes onto these materials, with an R^2 of 0.99954 for the CNT-N-ox and an R^2 of 0.98455 for the CNF-ox. When analyzing the isotherms of both materials (Fig. 4), CNT-N-ox showed a q_{max} of 22.7 mg/g, while CNF-ox showed a superior q_{max} value of 30.7 mg/g. The comparison of the maximum RNA adsorption capacity of these materials with values obtained in other studies involving nanoparticles for RNA adsorption, it is possible to observe that both of these materials exhibit RNA adsorption capacities similar to those studies (between 16 and 74.6 mg/g) [15,21,29]. While the adsorption capacity of the materials in the study may be slightly lower, an advantage lies in the ease of recovering the adsorbed RNA from these oxidized materials. Additionally, these materials are capable of achieving efficient capture of RNA in a simple and relatively rapid manner.

3.1.4. RNA desorption

The results indicated that exploring hydrophobic interactions was the most suitable option to promote the adsorption of RNA over CNT-N-ox and CNF-ox. The use of 10 mM Tris-HCl buffer at pH 8 was relatively effective in recovering RNA from the materials (Fig. 2). However, to provide a more comprehensive understanding of the potential for RNA recovery from these materials, additional elution buffers were examined. These experiments involved altering both the buffer composition and pH conditions. Specifically, the pH of the Tris-HCl buffer was raised to pH 9, and conversely, a 100 mM Acetate buffer at pH 5 was employed. Furthermore, surfactants, specifically 0.01 % Tween-20 and 0.2 % Triton X-100, were also introduced.

Except for the use of the 100 mM acetate buffer pH 5, there was an increase in the percentage of RNA desorption for both materials when compared with the desorption obtained with the 10 mM Tris-HCl buffer pH 8 (Fig. 5). A noticeable improvement in the desorption yield was observed at higher pH values, such as pH 9. This can be attributed to some differences in the ionization degree of all species involved in the adsorption process, resulting in enhanced negative charge on both the RNA and the polar groups of CNT-N-ox and CNF-ox. The increased charge repulsion weakens the electrostatic interactions between the negatively charged RNA and the adsorbent surfaces. While pH 8 is commonly employed in RNA elution protocols, it may not generate sufficient charge repulsion to fully release RNA from the adsorbent, leading to lower desorption efficiency. For both materials, the best RNA desorption was obtained with the 0.2 % Triton X-100 buffer, with 95.2 % and 85.8 % of RNA recovery from CNT-N-ox and CNF-ox, respectively. However, since the percentages of RNA desorption with 10 mM Tris-HCl, pH 9 (81 % for N-doped CNT-N-ox and 72.5 % for CNF-ox) were not very different from the percentages obtained with Triton X-100, the Tris-HCl buffer was the selected condition, to avoid the incorporation of surfactants. With this strategy and avoiding the addition of surfactants, it is most likely that the RNA integrity is preserved. Moreover, it is not expected a significant influence on the RNA adsorption capacity when reusing these materials in new cycles due to the non-specific adsorption of surfactants to carbon materials, as described in the literature [25,35].

3.2. Reuse of carbon materials

The reusability of the CNT-N-ox and CNF-ox was also addressed. Since almost complete RNA desorption was confirmed when the appropriate elution buffer (10 mM Tris-HCl pH 9) was applied, it was expected that after a new RNA capture cycle, the RNA adsorption capacity of the materials would be maintained or not be significantly changed. Thus, the application of this RNA desorption buffer was evaluated as a desorption strategy and a regeneration procedure for the materials under study. Therefore, for both materials, the previously used RNA capture method was applied, and after the desorption, a washing step was carried out with deionized water to repeat the adsorption/desorption experiments over 4 cycles. The results of these assays for the 2 materials are shown in Fig. 6. Looking at Fig. 6, it can be concluded that over the 4 cycles, there was a slight loss, of around 13 %, of RNA adsorption capacity by the CNT-N-ox, which is considered a promising result. On the other hand, some loss of RNA adsorption was observed after the 1st cycle of CNF-ox, resulting in nearly a 30 % reduction in adsorption capacity by the end of the 4th cycle. Thus, it is concluded that despite some loss of capacity to capture RNA, both materials showed a good capacity to be reused, making this process more efficient and environmentally friendly. In this context, the attention turns to exploring the feasibility of employing these materials for enhanced purification in the presence of a complex sample over several cycles, as described in the preceding chapters.

3.3. Selectivity between RNA and pDNA

To evaluate the ability of the carbon materials to separate RNA from impurities, selectivity assays between RNA and pDNA were performed to understand the influence that the presence of pDNA may have on RNA capture. For these experiments, 3 different ratios of RNA and pDNA were prepared, namely 1:1 (RNA/pDNA), 1:2 (RNA/pDNA), and 2:1 (RNA/pDNA). For this and considering the maximum RNA adsorption capacities of the materials, the mixtures were prepared with the following final concentrations: 20 μg/mL + 20 μg/mL (RNA/pDNA), 30 μg/mL + 30 μg/mL (RNA/pDNA), 20 μg/mL + 40 μg/mL (RNA/pDNA) and 20 μg/mL + 10 μg/mL (RNA/pDNA).

Considering the representative agarose gel electrophoresis of the CNT-N-ox (Fig. 7), it was possible to observe that for all tested ratios, part of the RNA is adsorbed while apparently most of the DNA remains in solution. This preferential adsorption of the RNA can occur because DNA is characterized by a compact structure with limited spatial

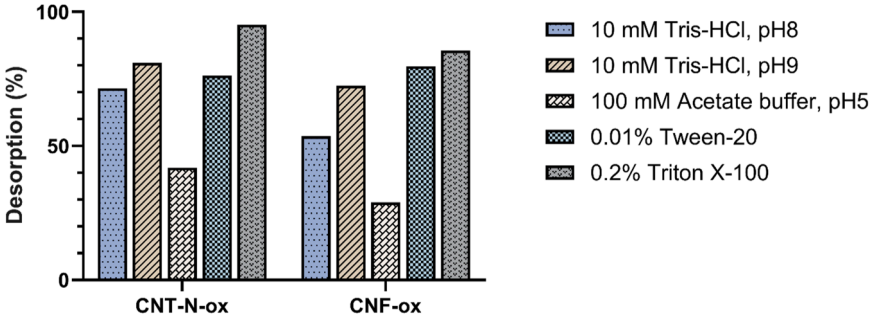

Fig. 5. RNA desorption from CNT-N-ox and from CNF-ox, using different desorption solutions.

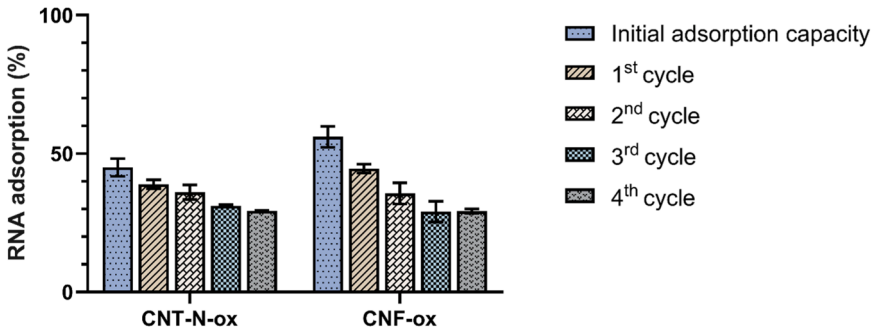

Fig. 6. RNA adsorption capacity of CNT-N-ox and CNF-ox over 4 cycles, using the 10 mM Tris-HCl, pH 9 buffer for desorption between each reusability cycle. Values were calculated with the data obtained from two independent measurements (mean ± SD, n = 4).

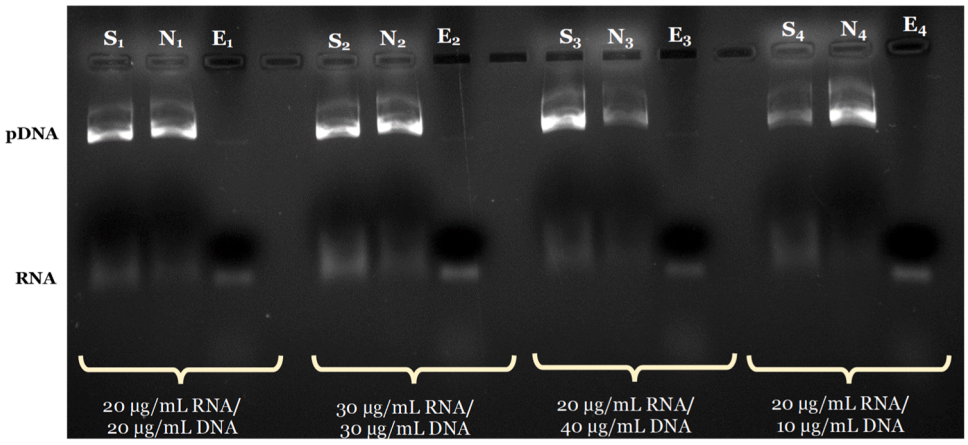

Fig. 7. Agarose gel electrophoresis of RNA and DNA mixtures before and after capture with CNT-N-ox, using 4 different ratios. S – Initial sample; N – Non-adsorbed fraction after incubation with CNT-N-ox; E – Species desorbed from CNT-N-ox. The plasmid pBHSR1-RM has 4.1 kbp, and the sRNA used ranges between 50 and 300 nucleotides.

availability of nitrogenous bases, contrary to RNA, which presents the nitrogenous bases much more exposed, enabling a higher interaction with the CNTs [31]. When analyzing the bands corresponding to the desorbed fraction, it was clear that the bands corresponding to the RNA were quite visible, while the DNA bands were practically unnoticed. Even when a higher concentration of DNA is present in the sample (40 µg/mL), the band corresponding to the RNA in the non-bound sample was almost inexistent, inferring that there was selectivity of the CNT-N-ox towards RNA. Although the materials did not capture the total RNA fraction, they considerably contributed to the clarification of pDNA in the non-bound sample for all RNA/DNA ratios while recovering an enriched sample of RNA in the desorbed fraction. In Fig. 8, which represents the agarose gel electrophoresis for the CNF-ox, it was possible to observe a very similar behavior to CNT-N-ox. It should also be noted that for all the RNA and DNA ratios under study, there was a higher RNA adsorption by the fibers, when compared with the CNTs, corroborating

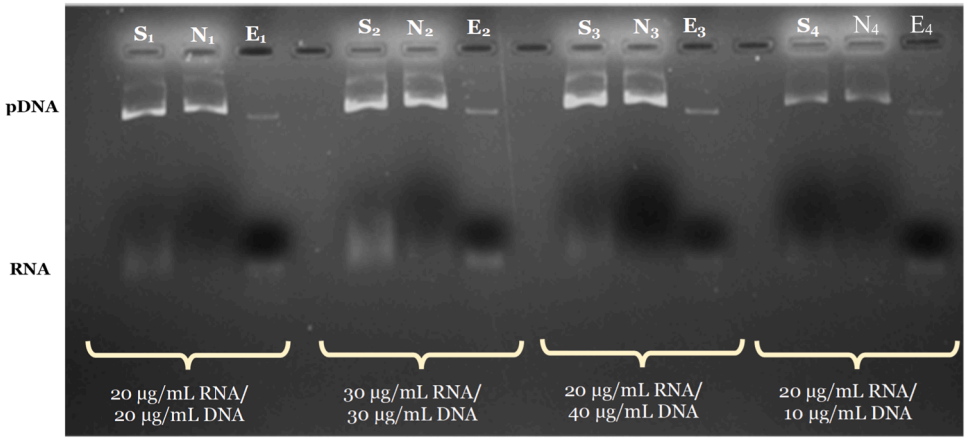

Fig. 8. Agarose gel electrophoresis of RNA and DNA mixtures before and after capture with CNF-ox, using 4 different ratios. S – Initial sample; N – Non-adsorbed fraction after incubation with CNF-ox; E – Species desorbed from CNF-ox. The plasmid pBHSR1-RM has 4.1 kbp, and the sRNA used ranges between 50 and 300 nucleotides.

the results obtained for the maximum RNA adsorption capacity. Additionally, CNF-ox exhibited some nonspecific adsorption of pDNA when compared to CNT-N-ox.

3.4. RNA adsorption from a lysate sample

To evaluate the performance of the materials in RNA capture and recovery from a complex sample, as well as to investigate the selectivity between RNA and other contaminating biomolecules, an *E. coli* lysate transformed with plasmid pBHSR1-RM sample was used. In this case, both materials were used over 3 consecutive cycles, i.e., the initial sample used in the 1st cycle corresponded to the lysate sample, and then the supernatant resulting from the 1st cycle was applied in a 2nd cycle, and the sample resulting from the 2nd cycle was finally applied in a 3rd cycle. The supernatants corresponding to each cycle were collected, as well as the desorbed RNA fractions, for further analysis by agarose gel electrophoresis and absorbance measurement, as shown in Fig. 9.

The analysis of the agarose gel electrophoresis of the experiment performed in CNT-N-ox (Fig. 9A) revealed that compared to the initial lysate sample (Fig. 9A S_1), there was a decrease in the intensity of the RNA band in the non-adsorbed fraction, after each cycle. More importantly, the analysis of the RNA bands corresponding to the desorbed fractions (Fig. 9A D_1, D_2, D_3), evidences the recovery of RNA after the 3 cycles without the presence of contaminating DNA. This result proved to be highly promising as it enabled the immediate recovery of RNA, without any DNA presence, just after the 1st cycle (Fig. 9A D_1). This not only underscores the selectivity of the material but also indicates an apparent clarification of the recovered RNA, representing a remarkable advance for the pre-purification of this biomolecule.

On the other hand, observing the agarose gel electrophoresis relative to the assays with the CNF-ox (Fig. 9B), it is possible to observe that, similarly to the CNTs, there was a decrease in the intensity of the RNA band, in the non-adsorbed fraction, after each cycle compared to the initial lysate sample. When analyzing the desorbed RNA band after the 1st cycle (Fig. 9B D_1), the possibility of recovering a considerable amount of RNA was verified, despite the presence of a slight contamination with DNA. Interestingly, when analyzing the following cycles (Fig. 9B D_2, D_3), it was observed the continuous recovery of RNA, while the DNA band decreased in intensity, apparently remaining in minimal amounts. Thus, compared to CNTs, the fibers required more than 1 cycle for the recovery of RNA free of large amounts of DNA, suggesting a lower selectivity.

To further confirm the selectivity towards RNA, and since pDNA is much longer than the sRNA used in the study, two additional assays were performed using the pUC19 vector (2.7 kbp), which is a smaller plasmid, and a linearized version of the plasmid. These assays aimed to evaluate whether the carbon materials selectivity depends on the length or structural configuration of the DNA. The results of these experiments confirmed that no adsorption of pDNA was observed when using an *E. coli* lysate sample with pUC19 plasmid for both materials (Figure S2), as well as no unspecific pDNA adsorption by the CNT-N-ox, while using linearized pUC19 plasmid (Figure S3). These findings are consistent with the earlier observations using larger plasmid DNA and further support the hypothesis that the selectivity of the material for RNA is driven by differences in nucleobase accessibility rather than the length or structural configuration of the nucleic acids.

Therefore, using the method described for these carbon materials, it was possible to capture and recover RNA from a lysate sample without the need to use the substantial quantities of toxic solvents typically employed in traditional RNA isolation techniques. In addition, the method used in this work is neither time-consuming nor highly operator-dependent. All these factors collectively contribute to the capability of this method to isolate RNA that is both biologically active and chemically stable.

3.5. Host proteins quantification

Proteins are a significant component of the *E. coli* host and represent one of the primary impurities associated with the RNA isolation process. In particular, it is known that *E. coli* comprises about 4300 protein-coding genes and that, according to FDA recommendations, the maximum level of protein in a biopharmaceutical product should preferably be less than 1 % (weight of impurity/weight of plasmid) [13]. For these reasons, the removal of these biomolecules is very important to

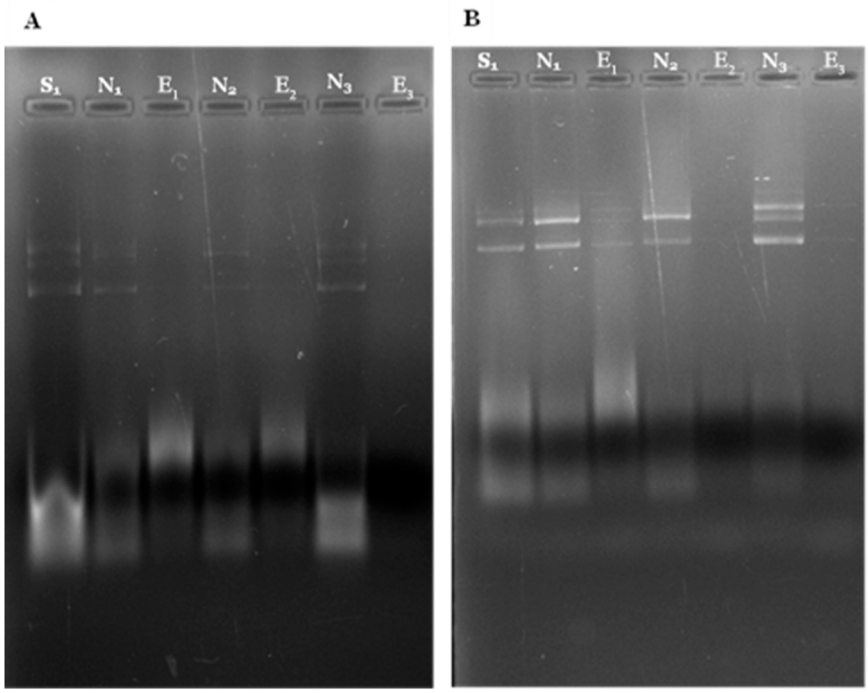

Fig. 9. Agarose gel electrophoresis of *E. coli* lysate before and after capture method for 3 consecutive cycles. A. CNT-N-ox; B. CNF-ox. S_1 – Initial *E. coli* lysate samples; N – Non-adsorbed fraction after incubation with (A) CNT-N-ox, and (B) CNF-ox; E – Species desorbed from (A) CNT-N-ox and (B) CNF-ox.

prevent possible immunogenic responses upon administration of biopharmaceuticals. In this regard, protein quantification was performed using the Bradford protein assay on the *E. coli* lysate sample and the samples recovered from the previous experiment of the 3 consecutive cycles. With the CNT-N-ox, from the 105 μg/mL of protein present in the initial *E. coli* lysate sample, none was detected in the non-adsorbed fraction after the 1st cycle, meaning that all protein was adsorbed. However, no protein was detected in the desorbed fraction, and throughout the subsequential remaining adsorption/desorption cycles. A similar trend was observed with the carbon fibers oxidized with HNO_3. From the 101 μg/mL of protein present in the initial *E. coli* lysate sample, 38 μg/mL was detected in the 1st non-adsorbed fraction, but no protein was detected in the desorbed fraction and throughout subsequential adsorption/desorption cycles. Analyzing the results obtained for the CNT-N-ox, they suggest that there is full protein capture as early as the 1st cycle. In fact, a study by Burch and co-workers demonstrated the remarkable ability of N-doped MWCNTs oxidized with H_2SO_4 and HNO_3 to capture metalloproteins. The observations from that study suggest that the proteins capture was mainly due to the hydrophilic nature of the amino acid side chains present on the outer surface of the proteins, which allows them to interact with the hydrophilic domains present on the oxidized surface of the material [7]. Moreover, the formation of hydrogen bonds between these chains and the carboxyl moieties on the surface of the MWCNTs could facilitate the stable adsorption of the proteins. Additionally, doping the MWCNTs with nitrogen enhanced the hydrophilicity of the material, further facilitating the interaction with the proteins and improving the capture of the metalloproteins [7]. This study then proposes an explanation for the full capture of the proteins present in the lysate sample by CNT-N-ox. In our case, also interesting was the fact that in the desorbed RNA sample, no protein is present, thus showing a 100 % protein reduction on the RNA desorbed sample compared to the initial lysate sample. This phenomenon is also in agreement with the work of Burch and co-workers, who described that metalloproteins remained adsorbed to the MWCNTs despite the application of washing and centrifugation steps, indicating strong interactions between the proteins and the material [7]. Overall, the results suggest that the desorption step is effective in RNA recovery, but proteins remain bound, which is very important to guarantee the clarification of the RNA sample.

Regarding CNF-ox, the results obtained indicate that in the 1st adsorption cycle, there was a significant protein capture, corresponding to a 63 % protein reduction in comparison with the initial lysate sample. Although there are no studies in the literature that elucidate the interaction between proteins and carbon fibers, this interaction is likely based on the same interactions that occurred for CNT-N-ox, since carbon fibers present similar surface chemistry and surface area. Still, the carbon fibers showed a lower capacity to capture proteins. On the other hand, there was also no presence of proteins in the sample desorbed after the 1st cycle, demonstrating once again the strong interactions occurring between the surface of the material and the proteins. It can also be seen that at the end of the 2nd cycle, it was possible to capture all the proteins that were present in the lysate sample, and again, no proteins were detected in the desorbed fraction. These results proved to be very auspicious as it was possible to recover RNA samples without the presence of proteins, which correspond to one of the main impurities in a lysate sample, concluding that both materials maintained their performance in reducing protein levels throughout all the trials.

3.6. RNA integrity after the capture and recovery from carbon materials

To evaluate the integrity and stability of the RNA recovered from CNT-N-ox and from CNF-ox, circular dichroism (CD) analysis was performed. For comparison purposes, a control sample of low molecular weight RNA was used and compared with the spectra of the RNA recovered from both materials after performing the proposed method (Fig. 10). Analyzing Fig. 10A, it can be seen that both spectra have similar profiles, with a negative band at 215 nm and a positive band at 265 nm, which are the characteristic bands of a typical RNA spectrum. The same behavior is seen in Fig. 10B where there are no significant differences in the characteristic RNA bands. These results indicate that there were no relevant alterations in the structure of the RNA during the process of clarification with carbon materials. Therefore, the RNA capture method applied in this work, using these materials does not compromise the integrity of the RNA, allowing it to maintain its native conformation.

4. Conclusion

In recent years, the discovery and understanding of the different RNA functions have increased drastically, providing several avenues to explore this biomolecule as a diagnosis or therapeutic agent. The unquestionable success of mRNA vaccines for the treatment of COVID-19 has opened horizons and shown the versatility of RNA-based therapies. The demand for RNA for the treatment of various diseases and, more recently, for vaccine development has increased exponentially. Thus, a widespread need arises to optimize the purification processes to obtain RNA with full integrity, highly pure, and biologically active. To address this challenge, different carbon materials differing in dimension, shape, and surface modifications were explored as a promising alternative for RNA capture and recovery from a complex sample. Common

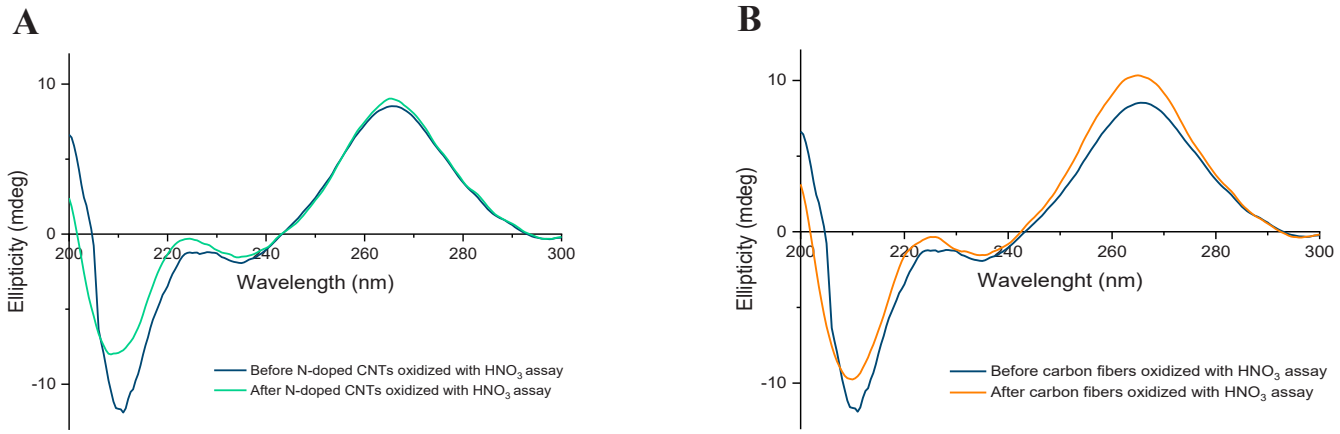

Fig. 10. A. CD spectra, from 200 to 300 nm, of RNA before and after capture assay with CNT-N-ox. The dark blue line represents control RNA before the capture procedure, and the green blue line represents RNA after the desorption procedure. **B.** CD spectra, from 200 to 320 nm, of RNA before and after capture assay with CNF-ox. The dark blue line represents control RNA before the capture procedure, and the orange line represents RNA after the desorption procedure.

RNA extraction methods present some limitations, such as time-consuming and complex procedures and the use of organic solvents that can compromise product integrity and have a negative environmental impact and low efficiency. In this work, it is proposed an alternative to surpass some of these challenges, by applying a fast, efficient, reliable, and cost-effective method that takes advantage of the notable adsorptive capabilities of carbon materials for RNA capture. This method can be seen as a pre-purification step and can be integrated into a biotechnological process to reduce impurities such as DNA and proteins.

CNT-N-ox and CNF-ox were the most promising carbon materials, exhibiting RNA adsorption percentages of 42 % and 55 %, respectively, and RNA desorption percentages of 81 % and 72 %, respectively. Subsequent experiments with these materials proved their ability to maintain RNA adsorption capacity over multiple cycles. Furthermore, when brought into contact with complex samples, the CNT-N-ox proved to be able to capture RNA with higher selectivity compared to CNF-ox. However, both materials were able to recover RNA without the presence of DNA over 3 cycles. Both materials under study were also able to fully capture the proteins present in the lysate sample, without compromising RNA desorption in the final recovery step. More importantly, it only required 1 extraction cycle for the CNT-N-ox to capture all proteins. Finally, circular dichroism experiments confirmed the integrity and stability of the RNA recovered from both materials.

Altogether, this work shows the applicability of a simple, rapid, and environmentally friendly method for efficient capture and pre-purification of RNA from bacterial lysates by exploiting the notable potential of carbon materials. This work may contribute positively to future investigations based on RNA extraction methods using carbon nanotubes and other carbon-based materials. While the materials used in this study have shown to be effective in capturing RNA, it would also be worth exploring other carbon materials and surface functionalization methods that could present higher adsorption capacity.

Funding

The authors acknowledge the projects UIDB/00709/2020, UIDP/00709/2020. This work was also financially supported by the national funds through FCT/MCTES (PIDDAC): LSRE-LCM, UIDB/50020/2020 (DOI: 10.54499/UIDB/50020/2020) and UIDP/50020/2020 (DOI: 10.54499/UIDP/50020/2020); ALiCE, LA/P/0045/2020 (DOI: 10.54499/LA/P/0045/2020), funded by national funds through FCT/MCTES (PIDDAC). MJS acknowledges FCT funding under the Scientific Employment Stimulus - Institutional Call (CEECINST/00010/2021/CP1770/CT0011). PLF acknowledges FCT for the PhD fellowships (2022.13803.BD).

CRediT authorship contribution statement

Ana Videira: Writing – original draft, Methodology, Investigation, Conceptualization. **Joaquim Faria:** Writing – review & editing, Resources, Methodology, Funding acquisition, Conceptualization. **Philippe Serp:** Writing – review & editing, Resources, Methodology, Conceptualization. **Maria Sampaio:** Writing – review & editing, Resources, Methodology, Conceptualization. **Pedro Ferreira:** Writing – original draft, Validation, Methodology, Investigation, Conceptualization. **Fani Sousa:** Writing – review & editing, Supervision, Resources, Project administration, Methodology, Funding acquisition, Conceptualization. **Cláudia Silva:** Writing – review & editing, Supervision, Resources, Project administration, Methodology, Funding acquisition, Conceptualization.

Declaration of Competing Interest

The authors declare that they have no known competing financial interests or personal relationships that could have appeared to influence the work reported in this paper

Appendix A. Supporting information

Supplementary data associated with this article can be found in the online version at doi:10.1016/j.colsurfa.2024.135532.

Data availability

Data will be made available on request.

References

[1] N. Ali, R.C.P. Rampazzo, A.D.T. Costa, M.A. Krieger, Current nucleic acid extraction methods and their implications to point-of-care diagnostics, Biomed. Res Int 2017 (2017) 9306564.
[2] M.R. Almeida, R.A.M. Barros, M.M. Pereira, D. Castro, J.L. Faria, M.G. Freire, C. G. Silva, A.P.M. Tavares, Multi-walled carbon nanotubes as a platform for immunoglobulin G attachment, Chem. Eng. Process. - Process. Intensif. 183 (2023) 109214.
[3] R. Arenal, K. March, C.P. Ewels, X. Rocquefelte, M. Kociak, A. Loiseau, O. Stéphan, Atomic configuration of nitrogen-doped single-walled carbon nanotubes, Nano Lett. 14 (2014) 5509–5516.
[4] B. Baptista, M. Riscado, J.A. Queiroz, C. Pichon, F. Sousa, Non-coding RNAs: emerging from the discovery to therapeutic applications, Biochem. Pharmacol. 189 (2021) 114469.
[5] L. Baronti, H. Karlsson, M. Marušič, K. Petzold, A guide to large-scale RNA sample preparation, Anal. Bioanal. Chem. 410 (2018) 3239–3252.
[6] C.P. Bergmann, F.M. Machado, Carbon nanomaterials as adsorbents for environmental and biological applications. Carbon Nanomaterials As Adsorbents For Environmental And Biological Applications, Springer International Publishing, 2015.
[7] H.J. Burch, S.A. Contera, M.R. De Planque, N. Grobert, J.F. Ryan, Doping of carbon nanotubes with nitrogen improves protein coverage whilst retaining correct conformation, Nanotechnology 19 (2008) 384001.
[8] R. Carapito, S.C. Bernardo, M.M. Pereira, M.C. Neves, M.G. Freire, F. Sousa, Multimodal ionic liquid-based chromatographic supports for an effective RNA purification, Sep. Purif. Technol. 315 (2023) 123676.
[9] P. Chomczynski, N. Sacchi, Single-Step Method Of Rna Isolation By Acid Guanidinium Thiocyanate-Phenol-Chloroform Extraction, Anal. Biochem 162 (1987) 156–159.
[10] P. Chomczynski, N. Sacchi, The single-step method Of RNA isolation by acid guanidinium thiocyanate–phenol–chloroform extraction: twenty-something years on, Nat. Protoc. 1 (2006) 581–585.
[11] M.M. Diogo, J.A. Queiroz, G.A. Monteiro, S.A.M. Martins, G.N.M. Ferreira, D.M. F. Prazeres, Purification of a cystic fibrosis plasmid vector for gene therapy using hydrophobic interaction chromatography, Biotechnol. Bioeng. 68 (2000) 576–583.
[12] S. Ethaib, S. Al-Qutaifia, N. Al-Ansari, S.L. Zubaidi, Function of nanomaterials in removing heavy metals for water and wastewater remediation: a review, Environments 9 (2022) 123.
[13] FDA, F.A.D.A. 2007. Guidance For Industry: Considerations For Plasmid Dna Vaccines For Infectious Disease Indications In: Services, U. S. D. O. H. A. H. (Ed.). Freedom Of Information Staff, (Hfi 35), Food And Drug Administration, Rm. 12 A - 30, 5600 Fishers Lane, Rockville, Md 20857, Usa, ⟨Http://Www.Fda.Gov/⟩, ⟨Http://Www.Fda.Gov/Downloads/Biologicsbloodvaccines/Guidancecomplianceregulatoryinformation/Guidances/Vaccines/Ucm091968.Pdf⟩.
[14] P. Ferreira, M. Riscado, S. Bernardo, M.G. Freire, J.L. Faria, A.P.M. Tavares, C. G. Silva, F. Sousa, Pristine multi-walled carbon nanotubes for a rapid and efficient plasmid DNA clarification, Sep. Purif. Technol. 320 (2023) 124224.
[15] Y. Fu, Q. Chen, L. Jia, Rnase-free RNA removal and dna purification by functionalized magnetic particles, Sep. Purif. Technol. 267 (2021) 118616.
[16] C.H. Giles, T.H. Macewan, S.N. Nakhwa, D. Smith, 786. Studies in adsorption. Part Xi. A system of classification of solution adsorption isotherms, and its use in diagnosis of adsorption mechanisms and in measurement of specific surface areas of solids, J. Chem. Soc. (1960) 3973–3993.
[17] B.J. Groenenberg, The chemistry of soils, in: Garrison Sposito (Ed.), 3rd ed., Oxford University Press, 2016. Hardback, pp. 272. Price Gbp 59.00, Eur 216.00. Isbn 9780190630881, John Wiley & Sons Limited.
[18] R.F. Hamilton, C. Xiang Jr., M. Li, I. Ka, F. Yang, D. Ma, D.W. Porter, N. Wu, A. Holian, Purification and sidewall functionalization of multiwalled carbon nanotubes and resulting bioactivity in two macrophage models, Inhal. Toxicol. 25 (2013) 199–210.
[19] P.K. Jiwanti, B.Y. Wardhana, L.G. Sutanto, D.M. Dewi, I.Z. Putri, I.N. Savitri, Recent development of nano-carbon material in pharmaceutical application: a review, Molecules 27 (2022).
[20] A.F. Jozala, D.C. Geraldes, L.L. Tundisi, V.D.A. Feitosa, C.A. Breyer, S.L. Cardoso, P.G. Mazzola, L.D. Oliveira-Nascimento, C.D.O. Rangel-Yagui, P.D.O. Magalhães, M.A.D. Oliveira, A. Pessoa, Biopharmaceuticals from microorganisms: from production to purification, Braz. J. Microbiol. 47 (2016) 51–63.
[21] Ç. Kip, H. Gülüşür, E. Çelik, D.D. Usta, A. Tuncel, Isolation of RNA and Beta-Nad by phenylboronic acid functionalized, monodisperse-porous silica microspheres as

sorbent in batch and microfluidic boronate affinity systems, Colloids Surf. B Biointerfaces 174 (2019) 333–342.
[22] J. Lipfert, S. Doniach, R. Das, D. Herschlag, Understanding nucleic acid-ion interactions, Annu Rev. Biochem 83 (2014) 813–841.
[23] E. Pamula, P.G. Rouxhet, Bulk and surface chemical functionalities of type iii pan-based carbon fibres, Carbon 41 (2003) 1905–1915.
[24] P. Pereira, A.Q. Pedro, J. Tomás, C.J. Maia, J.A. Queiroz, A. Figueiras, F. Sousa, Advances in time course extracellular production of human pre-Mir-29b from Rhodovulum Sulfidophilum, Appl. Microbiol. Biotechnol. 100 (2016) 3723–3734.
[25] T.R. Pozegic, S. Huntley, M.L. Longana, S. He, R.M.I. Bandara, S.G. King, I. Hamerton, Improving dispersion of recycled discontinuous carbon fibres to increase fibre throughput in the Hiperdif process, Materials (2020) 13.
[26] A.D. Purceno, B.F. Machado, A.P.C. Teixeira, T.V. Medeiros, A. Benyounes, J. Beausoleil, H.C. Menezes, Z.L. Cardeal, R.M. Lago, P. Serp, Magnetic amphiphilic hybrid carbon nanotubes containing N-doped and undoped sections: powerful tensioactive nanostructures, Nanoscale 7 (2015) 294–300.
[27] M.M. Sabzehmeidani, S. Mahnaee, M. Ghaedi, H. Heidari, V.A.L. Roy, Carbon based materials: a review of adsorbents for inorganic and organic compounds, Mater. Adv. 2 (2021) 598–627.
[28] K. Sathya, K. Nagarajan, G. Carlin Geor Malar, S. Rajalakshmi, P. Raja Lakshmi, A comprehensive review on comparison among effluent treatment methods and modern methods of treatment of industrial wastewater effluent from different sources, Appl. Water Sci. 12 (2022) 70.
[29] S. Senel, Boronic acid carrying (2-Hydroxyethylmethacrylate)-based membranes for isolation of RNA, Colloids Surf. A Physicochem. Eng. Asp. 219 (2003) 17–23.
[30] P. Serp, Carbon nanotubes and nanofibers in catalysis, Carbon Mater. Catal. (2008).
[31] I.I. Shakhmaeva, E.R. Bulatov, O.V. Bondar, D.V. Saifullina, M. Culha, A. A. Rizvanov, T.I. Abdullin, Binding and purification of plasmid DNA using multi-layered carbon nanotubes, J. Biotechnol. 152 (2011) 102–107.
[32] J. Stadler, R. Lemmens, T. Nyhammar, Plasmid DNA purification, J. Gene Med. 6 (2004) S54–S66.
[33] S.C. Tan, B.C. Yiap, DNA, RNA, and protein extraction: the past and the present, J. Biomed. Biotechnol. 2009 (2009) 574398.
[34] S.C. Tan, B.C. Yiap, DNA, RNA, and protein extraction: the past and the present, Biomed Research International, 2009, 2009574398.
[35] L. Vaisman, H.D. Wagner, G. Marom, The role of surfactants in dispersion of carbon nanotubes, Adv. Colloid Interface Sci. 128-130 (2006) 37–46.
[36] I. Vomelova, Z. Vaníčková, A. Šedo, Technical note methods of RNA purification. All Ways (Should) Lead To Rome, Folia Biol. (Praha) 55 (2009) 243–251.